PCCP

Cite this: *Phys. Chem. Chem. Phys.*, 2011, **13**, 6340–6351

www.rsc.org/pccp

PAPER

Ultrafast excited state dynamics and spectroscopy of 13,13′-diphenyl-β-carotene†‡

Kai Golibrzuch,[a] Florian Ehlers,[a] Mirko Scholz,[a] Rainer Oswald,[a] Thomas Lenzer,[b] Kawon Oum,*[b] Hyungjun Kim[c] and Sangho Koo*[c]

Received 13th November 2010, Accepted 8th February 2011
DOI: 10.1039/c0cp02525a

Ultrafast transient broadband absorption spectroscopy based on the Pump–Supercontinuum Probe (PSCP) technique has been applied to characterize the excited state dynamics of the newly-synthesized artificial β-carotene derivative 13,13′-diphenyl-β-carotene in the wavelength range 340–770 nm with *ca.* 60 fs cross-correlation time after excitation to the S_2 state. The influence of phenyl substitution at the polyene backbone has been investigated in different solvents by comparing the dynamics of the internal conversion (IC) processes $S_2 \rightarrow S_1$ and $S_1 \rightarrow S_0$* with results for β-carotene. Global analysis provides IC time constants and also time-dependent S_1 spectra demonstrating vibrational relaxation processes. Intramolecular vibrational redistribution processes are accelerated by phenyl substitution and are also solvent-dependent. DFT and TDDFT-TDA calculations suggest that both phenyl rings prefer an orientation where their ring planes are almost perpendicular to the plane of the carotene backbone, largely decoupling them electronically from the polyene system. This is consistent with several experimental observations: the up-field chemical shift of adjacent hydrogen atoms by a ring-current effect of the phenyl groups in the ^{1}H NMR spectrum, a small red-shift of the $S_0 \rightarrow S_2(0–0)$ transition energy in the steady-state absorption spectrum relative to β-carotene, and almost the same $S_1 \rightarrow S_0$* IC time constant as in β-carotene, suggesting a similar S_1–S_0 energy gap. The oscillator strength of the $S_0 \rightarrow S_2$ transition of the diphenyl derivative is reduced by *ca.* 20%. In addition, we observe a highly structured ground state bleach combined with excited state absorption at longer wavelengths, which is typical for an "S* state". Both features can be clearly assigned to absorption of vibrationally hot molecules in the ground electronic state S_0* superimposed on the bleach of room temperature molecules S_0. The S_0* population is formed by IC from S_1. These findings are discussed in detail with respect to alternative interpretations previously reported in the literature. Understanding the dynamics of this type of artificial phenyl-substituted carotene systems appears useful regarding their future structural optimization with respect to enhanced thermal stability while keeping the desired photophysical properties.

1. Introduction

Carotenoids represent a diverse group of naturally occurring dye molecules and act as accessory light-harvesting pigments in the blue-green spectral region, where chlorophyll absorption is weak.[1] Carotenoids also protect against excessive light conditions through singlet–singlet energy transfer or by quenching both singlet and triplet states of bacteriochlorophylls. Apart from photosynthesis, carotenoids are found in virtually all living organisms and play a key role in protective mechanisms by quenching reactive oxygen species, which is most likely of high relevance to the defense against several diseases. Besides, carotenoids are of great importance in the food industry as coloring and anti-oxidizing agents and therefore synthesized on an industrial scale.[2]

Once a carotenoid molecule is one-photon excited to its bright $S_2(1^1B_u^+)$ state, the simple electronic relaxation

[a] *Georg-August-Universität Göttingen, Institut für Physikalische Chemie, Tammannstr. 6, 37077 Göttingen, Germany*
[b] *Universität Siegen, Physikalische Chemie, Adolf-Reichwein-Str. 2, 57076 Siegen, Germany. E-mail: oum@chemie.uni-siegen.de; Fax: +49 271 740 2805; Tel: +49 271 740 2803*
[c] *Department of Chemistry and Department of Nano Science and Engineering, Myong Ji University, San 38-2, Nam-Dong, Yongin, Kyunggi-Do, 449-728, Korea*

† Dedicated to Prof. Dr Jürgen Troe on the occasion of his 70th birthday.

‡ Electronic supplementary information (ESI) available: Details of the synthesis and ^{1}H NMR spectrum of 13,13′-diphenyl-β-carotene. Steady-state absorption spectra of 13,13′-diphenyl-β-carotene in several organic solvents. Results from DFT/TDDFT-TDA calculations for 13,13′-diphenyl-β-carotene and β-carotene: energy profiles for phenyl rotation in S_0, S_1 and S_2; tables containing gas-phase transition energies, transition wavelengths and oscillator strengths for the first five excited singlet states obtained using BLYP and SVWN functionals. See DOI: 10.1039/c0cp02525a

pathway $S_2(1^1B_u^+) \rightarrow S_1(2^1A_g^-) \rightarrow S_0(1^1A_g^-)$ is frequently assumed for interpreting the excited state dynamics and is consistent with many spectroscopic observations.[3] Typical lifetimes reported in the literature are roughly 100–200 fs for S_2 and a few to several hundred picoseconds for S_1 (depending mainly on the effective conjugation length). In addition, several other states have been suggested as potentially important intermediates, such as $1^1B_u^-$ and S*, yet their relevance in the excited-state network is currently hotly debated.[4–6] For instance, several interpretations regarding the origin of the S* state have been put forward, describing it either as an electronically excited state,[7–12] the vibrationally hot ground electronic state (S_0*)[6,13–16] or the vibrationally hot S_1 state.[17] In Section 4.6, we present an extended discussion of our current findings considering previous results.

Various questions regarding crucial details of the photophysical and structural properties of carotenoids are therefore still not resolved. One promising approach to obtain a better understanding of these issues are controlled systematic changes of the molecular structure, *e.g.* at the polyene backbone of natural C_{40} carotenoids, by appropriate synthesis methods, as carried out in the present paper. In this report, we have focused on a newly-synthesized artificial C_{40} carotenoid with two phenyl rings at the C_{13} and C_{13}' positions, namely 13,13′-diphenyl-β-carotene (see Fig. 1), which retains the same conjugated double bond polyene system as β-carotene. This way, one can study the influence of increased steric complexity and/or changes in electronic substituents on the energetic positions of the electronic states of these polyene systems and their photophysical properties. We present investigations of the steady-state spectroscopy and the ultrafast excited state dynamics of this modified β-carotene by employing ultrafast Pump–SuperContinuum-Probe (PSCP) broadband absorption spectroscopy covering the UV to the near IR range. We combine our experiments also with theoretical calculations based on DFT/TDDFT-TDA methods to obtain information on how the two phenyl substituents at the polyene backbone influence the molecular structure and the location, charge distribution and lifetime of the low-lying electronic states. The results of this study are also relevant to the development of artificial carotenoid-based systems with superior thermal and photochemical stability, which can *e.g.* be used as conducting molecular wires.[18]

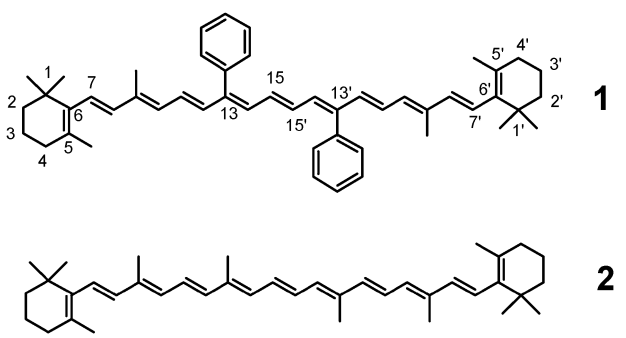

Fig. 1 Chemical structures of 13,13′-diphenyl-β-carotene (**1**) and β-carotene (**2**).

2. Experimental

2.1 Synthesis of 13,13′-diphenyl-β-carotene and its characterization

Synthesis of the novel 13,13′-diphenyl-β-carotene (**1**) was carried out by the application of the double elimination protocol to the coupling product between [(2*E*,4*E*)-3-methyl-5-(2,6,6-trimethylcyclohex-1-enyl)penta-2,4-dienylsulfonyl]benzene (**3**) and (*E*)-2,7-diphenyloct-4-enedial (**4**) (see ESI‡ for the numbering of compounds).[19] The lithium anion of the allylic sulfone **3**, which was prepared by treatment of *n*-BuLi, reacted with a half equivalent dial **4** in THF at −78 °C to produce the required carbon skeleton for the carotene **1**. The resulting diol functional groups of the coupling product **5** were protected as methoxymethyl (MOM) ethers, which then underwent double eliminations of benzenesulfonyl and MOM groups under refluxing conditions in cyclohexane/benzene (~5 : 1 *v* : *v*) using KOMe. The carotene **1** was purified by recrystallization and characterized to be all-*trans* configuration based on ^{1}H NMR analysis. The experimental details are included in the ESI.‡

Data for **1**: ^{1}H NMR δ 0.91 (s, 12H), 1.42–1.48 (m, 4H), 1.55–1.64 (m, 4H), 1.68 (s, 6H), 1.71 (s, 6H), 2.00 (dd, J = 6.4, 6.0 Hz, 4H), 6.08 (A of ABq, J = 16.4 Hz, 2H; H^7), 6.09 (B of ABq, J = 16.4 Hz, 2H; H^8), 6.11 (d, J = 10.6 Hz, 2H; H^{10}), 6.15–6.20 (m, 2H; H^{15}), 6.22 (dd, J = 14.4, 10.6 Hz, 2H; H^{11}), 6.24–6.28 (m, 2H; H^{14}), 6.43 (d, J = 14.4 Hz, 2H; H^{12}), 7.16–7.22 (m, 4H), 7.34–7.39 (m, 2H), 7.39–7.46 (m, 4H) ppm; ^{13}C NMR δ 15.7, 22.2, 24.7, 31.9, 31.9, 36.1, 37.2, 42.6, 130.0, 130.3, 131.2, 131.4, 132.5, 132.9, 133.7, 134.8, 135.4, 139,4, 139.7, 140.7, 140.8, 140.9, 146.4 ppm; IR (KBr) 3030, 2930, 1717, 1684, 1653, 1636 cm^{-1}; HRMS (FAB$^+$) calcd for $C_{50}H_{60}$ 660.4695, found 660.4691.

2.2 PSCP spectroscopy

A description of the setup and the principles of PSCP spectroscopy are given elsewhere.[20–22] Briefly, a Ti : sapphire oscillator-regenerative amplifier system delivered 780 nm pulses at a repetition frequency of 920 Hz with 100 fs pulse length at an energy of 1 mJ pulse^{-1}. This source was employed for the generation of ultrashort pump and probe pulses in two home-built NOPAs.[23,24] The pump NOPA was set to generate pulses at 485–500 nm. These were afterwards compressed by a quartz prism pair and then attenuated to excite the carotenes *via* their $S_0 \rightarrow S_2(0\text{–}0)$ transition. Photon densities of *ca.* 5×10^{14} cm^{-2} were employed for excitation. The output of the second NOPA was centered at 550 nm and passed through another identical compression stage before focusing it into a 1 mm thick CaF_2 plate for generation of a supercontinuum (range used in this study: 340–770 nm). The supercontinuum was spectrally filtered, and then split into a reference and sample path. Pump and probe pulses were overlapped in the flow cell (path length: 400 μm, window thickness: 200 μm) at magic-angle polarization. Two spectrographs with 512 element photodiode arrays were employed to detect the reference and sample beams. Transient spectra for each pump–probe delay represent the average of three independent scans (1500 shots total with single-shot baseline correction). In the experiments, the

pump–probe intensity cross-correlation time of the setup was between 55 and 62 fs and the time accuracy 10 fs. The transient signals were analyzed globally based on the kinetic scheme $S_2 \rightarrow S_1 \rightarrow S_0^* \rightarrow S_0$, where S_0^* is the intermediately formed vibrationally excited ground electronic state.[6,13–15] The modeling also included a possible time dependence for the individual spectra of the respective electronic states.[6,25] In the current study, such a time dependence was required to adequately describe relaxation processes in the S_1 state and collisional deactivation of S_0^* molecules, for details see Section 4.3. Time constants and spectral shapes were optimized simultaneously in an automated fashion during the fitting procedure.

3. Theoretical calculations

Briefly, the equilibrium structures of 13,13′-diphenyl-β-carotene and β-carotene in the ground electronic state were optimized by density functional theory (DFT) using the B3LYP functional[26] and a 6-311G** basis set. Subsequently, time-dependent density functional theory (TDDFT)[27,28] using the Tamm-Dancoff approximation (TDA)[29] was applied to these geometries for calculating the first five excited singlet electronic states at vertical excitation using the BLYP,[30a] B3LYP and SVWN[30b,c] functionals and a 6-31+G* basis set. Calculations were carried out using the Q-CHEM 3.0 package.[31] For a detailed discussion of known limits and drawbacks of TDDFT methods in the description of excited polyene electronic states see ref. 32.

4. Results and discussion

4.1 Electronic steady-state absorption spectroscopy

The upper panel of Fig. 2 shows a comparison of the steady-state absorption spectra of 13,13′-diphenyl-β-carotene (**1**) and β-carotene (**2**) in *n*-hexane. Assuming C_{2h} symmetry, one-photon absorption of carotenoids is symmetry-forbidden for $S_0(1^1A_g^-) \rightarrow S_1(2^1A_g^-)$, and the strong absorption in the blue–green region is therefore due to the $S_0(1^1A_g^-) \rightarrow S_2(1^1B_u^+)$ transition. We observed a red-shift of the absorption band for **1** relative to **2** in organic solvents: for example, in *n*-hexane, 414 cm^{-1} and 401 cm^{-1} for the 0–0 and 0–1 transitions, respectively. Similar red-shifts for **1** relative to **2** were observed in other organic solvents (acetone, THF, *i*-octane, toluene and CH_2Cl_2), and the extent of the red-shift was slightly dependent on the solvent (370–430 cm^{-1}). The widths of the absorption bands in Fig. 2 were similar for **1** (FWHM 3913 cm^{-1}) and **2** (4026 cm^{-1}). We note that the absorption coefficient at the spectral maximum of **1** was about 20% smaller than for **2** (1.32×10^5 for **1** and 1.72×10^5 L mol^{-1} cm^{-1} for **2** in CH_2Cl_2), resulting in an oscillator strength ratio of 0.78. For further details see Table S2 and Fig. S2 in the ESI.‡

The energetic position of the absorption band maximum of β-carotene correlates well with the Lorentz–Lorenz function $R(n) = (n^2 - 1)/(n^2 + 2)$ (n being the refractive index of the solvent).[33–35] This is attributed to dispersion effects due to the higher polarizability of S_2 compared with S_0.[33] The lower panel of Fig. 2 illustrates the absorption maxima of β-carotene

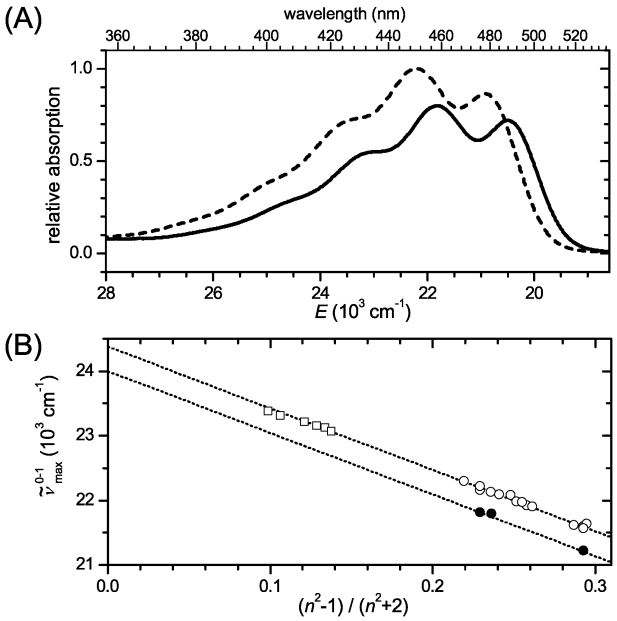

Fig. 2 (A) Comparison of steady-state absorption spectra of 13,13′-diphenyl-β-carotene (solid line) with β-carotene (dashed line). Both spectra were recorded in *n*-hexane at room temperature. The spectrum for β-carotene was normalized to one, and the spectrum of the 13,13′-derivative was rescaled so that the experimentally observed ratio of the absorption maxima was reproduced accordingly. (B) Absorption maxima ($\tilde{\nu}_{max}^{0-1}$ in cm^{-1}) as a function of the solvent polarizability function $R(n) = (n^2 - 1)/(n^2 + 2)$ in nonpolar solvents: (open circles) β-carotene in organic solvents, (open squares) β-carotene in supercritical CO_2 (from ref. 35 and references therein); (filled circles) 13,13′-diphenyl-β-carotene (nonpolar solvents of this work: *n*-hexane, *i*-octane and toluene). Dotted lines are linear fits to the experimental data points extrapolated to the respective gas-phase limits.

in nonpolar organic solvents ($R(n)$ = 0.20–0.35) and supercritical CO_2 ($R(n)$ = 0.10–0.15) employing eqn (1).[35] By extrapolating these values to $R(n) = 0$ one can estimate the gas-phase limit of the $S_0 \rightarrow S_2(0–1)$ transition of β-carotene[35]

$$\tilde{\nu}(S_0 \rightarrow S_2(0–1))\ (\mathbf{2}) = [24\,380 - 9431R(n)]\ cm^{-1} \qquad (1)$$

The estimated uncertainty for the gas-phase value of **2** is *ca.* 120 cm^{-1}. An analogous procedure can be applied for 13,13′-diphenyl-β-carotene. The extrapolation based on the three data points in *n*-hexane, *i*-octane and toluene (filled circles in the lower panel of Fig. 2) yields:

$$\tilde{\nu}(S_0 \rightarrow S_2(0–1))\ (\mathbf{1}) = [23\,980 - 9428R(n)]\ cm^{-1} \qquad (2)$$

Because currently no steady-state absorption data for **1** in supercritical fluids are available for the extrapolation, the uncertainty of the extrapolated gas-phase value is larger than for **2**, and we estimate it to be 300 cm^{-1}. We estimate the energy difference for the $S_0 \rightarrow S_2(0–1)$ transition of the two carotenes in the gas-phase limit to be 400 cm^{-1}. Similarly, we can determine the energy for the 0–0 transition by considering the spacing between the 0–0 and 0–1 peaks, for example 1300 cm^{-1} in *n*-hexane. This provides the energy of the $S_0 \rightarrow S_2(0–0)$ transition as 22 660 cm^{-1} (20 500 cm^{-1}) for 13,13′-diphenyl-β-carotene and 23 070 cm^{-1} (20 910 cm^{-1}) for β-carotene in the gas-phase (*n*-hexane).

The introduction of the two phenyls brings about a clear bathochromic shift. The *ca.* 400 cm^{-1} red-shift is less than what is found when adding an extra double bond to the conjugated polyene backbone.[36] This indicates that the two phenyl rings have a relatively weak influence on the conjugated system. As will be shown below, this is consistent with our other results from ultrafast excited state dynamics, the DFT/TDDFT-TDA calculations and also the ^{1}H-NMR data. Interestingly, in the experiment we find a *ca.* 20% reduction in oscillator strength upon phenyl substitution.

4.2 Transient PSCP spectra

Representative ultrafast broadband absorption spectra of **1** and **2** in acetone are shown in Fig. 3 and 4, respectively. The carotenes were excited at the $S_0 \rightarrow S_2(0–0)$ transition (485 nm). Additional PSCP spectra were recorded for **1** in *n*-hexane and **2** in THF (not shown), for transient PSCP spectra of **2** in *n*-hexane see ref. 6. Table 1 summarizes experimental conditions and kinetic information extracted from the PSCP spectra.

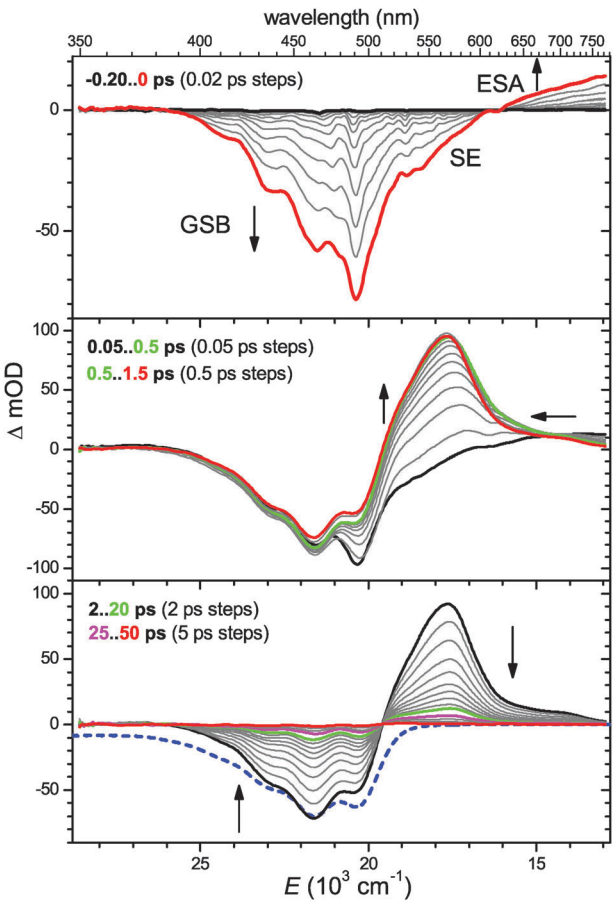

Fig. 3 Transient PSCP absorption spectra of 13,13′-diphenyl-β-carotene in acetone for excitation at 485 nm (cross correlation 59 fs): (upper panel) −0.2–0 ps with 20 fs steps; (middle panel) 0.05–0.50 ps and 0.50–1.50 ps with 50 fs and 500 fs steps, respectively; (lower panel) 2–20 ps and 25–50 ps with 2 ps and 5 ps steps, respectively. Some transient spectra are plotted as thick colored lines for guidance. For comparison, the inverted and scaled steady-state absorption spectrum is shown in the lower panel as a blue dashed line.

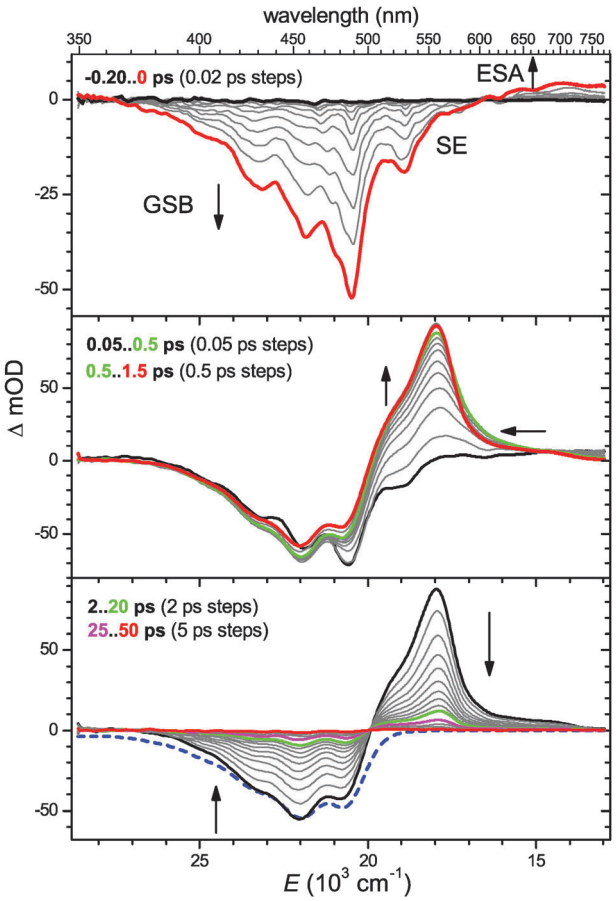

Fig. 4 Same as in Fig. 3 but for β-carotene in acetone: excitation at 485 nm, cross correlation 62 fs.

The top panel of Fig. 3 contains the evolution of the PSCP spectra between −0.20 and 0 ps (20 fs steps). At early times, negative ground state bleaching (GSB, $S_0 \rightarrow S_2$) and stimulated emission (SE, $S_2 \rightarrow S_0$) are developing. Raman structure of the carotene is superimposed and is more prominent on the anti-Stokes side. At the same time, transient excited state absorption (ESA) is formed above 620 nm, which is assigned to an $S_2 \rightarrow S_n$ transition. Similar observations are made for β-carotene in Fig. 4, however the whole spectrum is clearly blue-shifted.

The middle panel in Fig. 3 shows the further spectral evolution from 0.05 ps to 0.5 ps in 50 fs steps, and from 0.5 ps to 1.5 ps in 500 fs steps. A fast internal conversion (IC) from the S_2 to the S_1 state occurs (time constant 180 fs), characterized by the decay of the SE and ESA features of S_2 and the concomitant increase of the $S_1 \rightarrow S_n$ ESA band centered around 570 nm which has a weak shoulder at *ca.* 520 nm. There is additional spectral evolution of this band in the 600–700 nm region, appearing as a weak blue-shift and a slight narrowing on the red band edge: one can see this effect clearly by comparing the two spectra marked as green and red lines. The dynamics are due to relaxation processes in S_1, which will be discussed below. For β-carotene (Fig. 4), the whole spectrum is blue-shifted, and a sharper $S_1 \rightarrow S_n$ ESA band with a more pronounced blue shoulder is observed. Also, we note already here that the S_1 relaxation dynamics in the

Table 1 Summary of global analysis results for 13,13′-diphenyl-β-carotene (**1**) and β-carotene (**2**) in organic solvents

Carotene	Solvent	λ_{pump}/nm	τ_{CC}[a]/fs	$\tau(S_2 \rightarrow S_1)$[b]/fs	$\tau_{relax}(S_1)$[c]/fs	$\tau(S_1 \rightarrow S_0^*)$[b]/ps	$\tau(S_0^* \rightarrow S_0)$[d]/ps
1	Acetone	485	59	180	200	9.3	10.4
1	*n*-Hexane	485	60	170	390	9.2	10.4
2	Acetone	485	62	170	510	9.0	11.5
2	*n*-Hexane[e]	487	55	160	630	8.7	11.9
2	THF	500	59	160	560	9.1	10.4

[a] Pump–probe intensity cross-correlation of the experiment. [b] Internal conversion (IC) time constants. [c] Time constant for blue-shifting and narrowing of the $S_1 \rightarrow S_n$ ESA band. [d] Time constant for vibrational relaxation in the ground electronic state due to collisions with the solvent. [e] From ref. 6.

phenyl substituted carotene are accelerated substantially (by a factor of two) compared to β-carotene.

In the bottom panel of Fig. 3 and 4 (2–50 ps) we observe the decay of the $S_1 \rightarrow S_n$ ESA band and the concomitant filling-up of the GSB with a characteristic time constant of 9.3 ps (9.0 ps), see Table 1, due to the $S_1 \rightarrow S_0^*$ IC process. We note that there is almost no GSB and spectral development below 400 nm in any of the transient spectra, despite of the fact that there is a small amplitude of the steady-state absorption spectrum (blue dashed line) in this spectral region. Such an effect was previously observed for β-carotene in THF and *n*-hexane,[6,12a,37] adonixanthin in acetone[22] and macrocarotenes.[13] This feature therefore appears to be rather general for carotenes, and is most likely due to an overlapping $S_1 \rightarrow S_{n+1}$ ESA transition in the UV region.

4.3 Global kinetic analysis of PSCP data

We performed a global kinetic analysis for all systems based on the model $S_2 \rightarrow S_1 \rightarrow S_0^* \rightarrow S_0$. Relaxation processes of S_1 and S_0^* molecules were considered in terms of time-dependent spectra for the species involved. A time-independent S_2 spectrum suffices for β-carotenes because of its very short lifetime. At this point, we would like to briefly discuss, why this type of kinetic modeling has been used and is advantageous for describing the photoinduced dynamics of carotenes. Consider, as one example, models of the type $S_2 \rightarrow S_1^* \rightarrow S_1 \rightarrow S_0$ used previously to account for the presence of relaxation processes within S_1.[17,38] It is immediately clear that such a model cannot be an accurate representation of the photoinduced dynamics because a part of the S_1^* molecules also directly relax to S_0 by IC without populating the relaxed S_1. One could improve this by extending the kinetic scheme by another step $S_1^* \rightarrow S_0$ and assuming *e.g.* the same IC lifetime as for $S_1 \rightarrow S_0$. Still the major drawback then is that a *single static* spectrum is assigned to S_1^* which is physically unrealistic: It is obvious that, depending on the degree of intramolecular relaxation, the spectrum of S_1 must change with time. The same consideration also holds for vibrationally "hot" molecules in a given electronic state, where their population has a continuously varying spectrum depending on their internal vibrational excess energy,[39,40] as well as for excited electronic states exhibiting solvation dynamics, where *e.g.* the emission of an S_1 state having a large dipole moment shows a considerable transient red-shift, often accompanied by a corresponding transient blue-shift of S_1 ESA features, such as observed in terminally carbonyl-substituted carotenoids and other molecules.[25,41] One reasonable way to account for such effects is to introduce a time-dependence for the spectrum of a given electronic species. This way, effects such as *intra*-electronic-state dynamics and solvation are taken care of by the time-dependent spectrum, whereas the whole population in this electronic state is at the same time subject to *inter*-electronic-state relaxation due to *e.g.* IC. An approximation in such a treatment is that a single IC time constant is assigned to all molecules in the given electronic state, regardless of the degree of relaxation. It is well-known that *e.g.* IC time constants can change with molecular excess energy,[42] so the IC time constants from such a kinetic treatment should be interpreted as an average value for the whole population distribution. The concept of time-dependent spectra has been widely used in the modeling of band shifts in solvation dynamics[25,41,43] and is here applied to β-carotene derivatives.

During the kinetic modeling of the current study, no indications for the involvement of electronic states other than S_2, S_1 and S_0 have been found, which is in agreement with earlier studies on C_{40} carotenoids.[6,14,22,37,44–48] Specifically, we (and also others[37]) could not confirm the presence of several pronounced oscillations for β-carotene in *n*-hexane on ultrashort time scales, which was reported as indication for strong coupling with the $1^1B_u^-$ state.[49] For the cold S_0 species we used the steady-state $S_0 \rightarrow S_2$ absorption spectrum, which was kept fixed. The S_2, S_1 and S_0^* spectra were represented by a sum of Gaussian functions to accurately describe the transient PSCP features. As shown previously by us in temperature-dependent steady-state absorption experiments, vibrationally "hot" S_0^* carotene spectra are broader than the room temperature spectrum and show additional features at longer wavelengths.[6] The coherent Raman response of the carotenes was incorporated by a separate spectrum appearing and disappearing with the cross-correlation time. Weak contributions of the pure solvent around $t = 0$ were subtracted from the PSCP spectra prior to kinetic analysis.

Fig. 5 shows the optimized spectra for the different electronic species of 13,13′-diphenyl-β-carotene (top) and β-carotene (bottom). A time-independent spectrum was sufficient to describe the spectral features of S_2. It is characterized by stimulated emission in the 490–630 nm region. For β-carotene, this part of the transient PSCP spectrum resembles the inverted broadband fluorescence spectrum reported previously (considering a factor $1/\nu^2$).[37] In addition, we clearly see $S_2 \rightarrow S_n$ ESA to the red and blue of the SE. The S_1 spectra show a characteristic time dependence which will be discussed below. The hot transient S_0^* spectra will be dealt with later on.

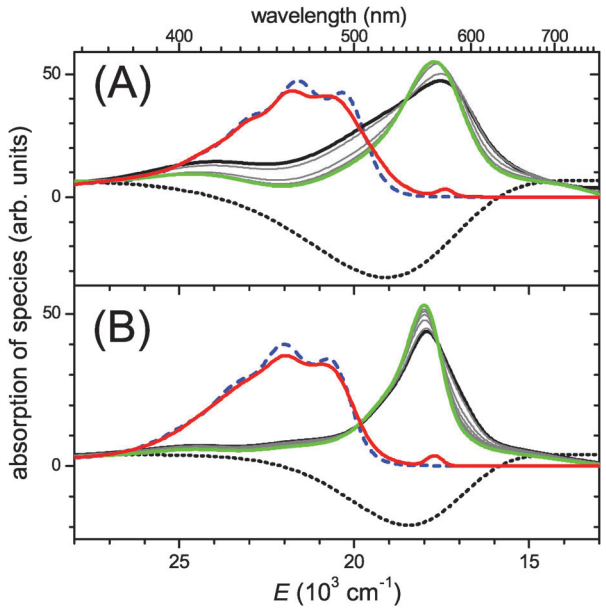

Fig. 5 Spectra of the different species obtained from global kinetic analysis for (A) 13,13′-diphenyl-β-carotene and (B) β-carotene in acetone, see Fig. 3 and 4 for the respective transient PSCP spectra. (Solid lines, right side): transient S_1 spectra at 0.15 (black line), 0.20, 0.40, 0.60, 0.80, 1.0 (grey lines) and 2.0 ps (green line). (Red solid line) S_0* spectrum at 15 ps. (Blue dashed line) steady-state absorption spectrum for S_0 at 298.15 K. (Black dotted line) spectrum of S_2.

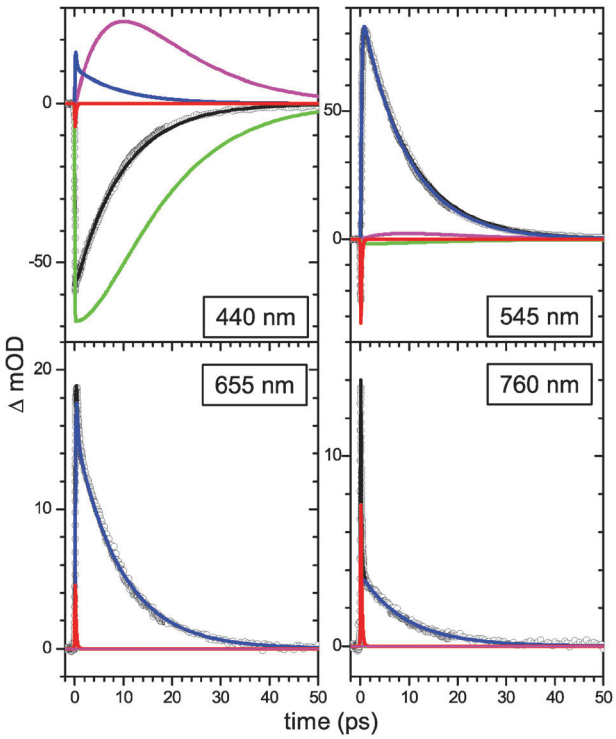

Fig. 6 Kinetic traces for 13,13′-diphenyl-β-carotene in acetone at four representative probe wavelengths (440, 545, 655 and 760 nm): (○) Experimental PSCP data from Fig. 3; (black line) simulation results from global kinetic analysis with individual contributions from S_2 (red line), S_1 (blue line), S_0* (magenta line) and S_0 (green line).

We extract a time constant of 180 fs for the $S_2 \rightarrow S_1$ decay of 13,13′-diphenyl-β-carotene in acetone and 170 fs for the corresponding experiment in *n*-hexane. The values are close to those of β-carotene: 170 fs in acetone (Fig. 4), 160 fs in *n*-hexane[6] and 160 fs in THF, the latter one being also in agreement with data from ref. 37. Similar observations were made for the $S_1 \rightarrow S_0$* IC time constant, which is known to be sensitive to the effective conjugation length.[3] It is practically identical and almost solvent-independent for both species: 9.3 and 9.2 ps for 13,13′-diphenyl-β-carotene in acetone and *n*-hexane, respectively, 9.0, 8.7 and 9.1 ps for β-carotene in acetone, *n*-hexane and THF, respectively. This observation leads us to one of the central questions of the current investigations: why is there only a weak influence on the IC lifetimes although the substitution on the polyene backbone has changed quite considerably? It appears as if there is almost no change in effective conjugation length when the 13,13′-substituents are changed from methyl to phenyl. We will address this point below with the aid of DFT/TDDFT-TDA calculations.

The 512 kinetic traces for all systems are well described by the global analysis, and four representative examples are found in Fig. 6 for 13,13′-diphenyl-β-carotene in acetone, representing the GSB (440 nm) and ESA regions (545, 655 and 760 nm). Each panel also shows the contributions of the individual species S_2 (red), S_1 (blue), S_0* (magenta) and S_0 (green).

4.4 Relaxation processes in S_1

We will now take a closer look at the time-dependence of the S_1 spectra in Fig. 5. For β-carotene, such a spectral change has been noticed previously.[6,38,50–54] We observe an analogous behavior for 13,13′-diphenyl-β-carotene, however on a much faster timescale.

Interestingly, the S_1 band of the diphenyl derivative is broader than for β-carotene. The spectral evolution is qualitatively similar. Our global analysis involving time-dependent S_1 spectra provides fine details of the narrowing and blue-shifting of the $S_1 \rightarrow S_n$ band. In both cases we find an isosbestic point (at *ca.* 585 nm for **1** and 570 nm for **2**). Notable is also a tail reaching into the UV, which is due to an additional weak $S_1 \rightarrow S_{n+1}$ transition. Most strikingly, S_1 relaxation of 13,13′-diphenyl-β-carotene is much faster (200 and 390 fs in acetone and *n*-hexane, respectively) than in β-carotene (510 and 630 fs). Also, relaxation in acetone is faster than in *n*-hexane. The value for β-carotene in *n*-hexane is in satisfactory agreement with the results of Mathies and co-workers in cyclohexane (400–470 fs) determined by femtosecond time-resolved stimulated Raman spectroscopy[53] and also transient absorption experiments.[14,52] The type of spectral evolution is consistent with intramolecular vibrational redistribution (IVR) processes in S_1 after IC from S_2 superimposed by considerably slower intermolecular energy transfer from S_1 to the solvent.

The results suggest that the IVR process in S_1 is influenced by intramolecular and intermolecular effects: The replacement of the two methyl groups by phenyls close to the center of the polyene backbone reduces the IVR time constant by about a factor of two. One reasonable interpretation could be that "rigid" torsions (methyls) are replaced by "floppy" torsions (phenyls) with lower vibrational frequency. Such types of

substitution are known to accelerate IVR.[55] In addition, the solvent can play an important role. For instance, in time-resolved pump–probe experiments on benzene in 1,1,2-trichloro-trifluoroethane and supercritical CO_2 a substantial dependence of IVR time constants on the type and density of the solvent was found.[56,57] In our case, acetone appears to be more efficient than *n*-hexane with respect to such "solvent-mediated" IVR. Also, the solvent effect appears to be more pronounced in the phenyl-substituted derivative than in β-carotene. It is still not well understood if static or dynamic solvent effects are responsible for the observed changes in IVR time constants.[56]

4.5 Relaxation of the S* state in β-carotene and its 13,13′-derivative

There has been considerable debate concerning the origin of the S* state features, and in Section 4.6 we will therefore separately discuss this issue in detail, especially with respect to very recent experiments by other groups, which favor the excited electronic state hypothesis for S*. Based on the arguments presented below, we are however sure that the S* state features in transient absorption spectra of carotenes can be unambiguously assigned to vibrationally hot S_0* molecules.[6] This must be then a general feature in ultrafast transient absorption experiments of carotenoids, because S_0* molecules are always produced upon IC from S_1. For instance, β-carotene molecules enter S_0 with an excess energy $\geq 14\,500$ cm^{-1},[3] corresponding to a vibrational temperature of >490 K.[6] In fact, the presence of this channel was already suggested in the pioneering experiments of Andersson and Gillbro for macrocarotenes.[13] Vibrationally excited S_0* molecules are also observed for 13,13′-diphenyl-β-carotene. Fig. 7 shows a comparison in the solvent acetone for 13,13′-diphenyl-β-carotene (A) and β-carotene (B). In both cases, PSCP spectra were averaged at long times (45–60 ps), when the S_1 state has largely decayed by IC and the remaining spectral signatures are governed by S_0*. Typical absorption of vibrationally excited molecules is seen above 500 nm. The highly structured bleach region is a consequence of the superposition of the S_0* absorption on the GSB of room-temperature S_0 molecules. Note that the transient S_0* spectrum of 13,13′-diphenyl-β-carotene is further shifted to the red, which is consistent with the clear shift in the room-temperature steady-state absorption spectrum (Fig. 2).

In the global analysis of the PSCP spectra, S_0* can already be well described by a time-independent hot absorption spectrum. S_0* appears with the IC time constant of S_1 and decays with a time constant of 10–12 ps, depending on the collisional energy transfer efficiency of the solvent. Still, with a time-independent S_0* spectrum, there remain small systematic differences, specifically in the hot band region between 500 and 600 nm. For instance, the absorption in this spectral region is slightly underestimated in the 5–15 ps region. Such deviations are expected because "hot" spectra in general narrow upon cooling. An almost perfect fit can therefore be obtained by including a time dependence of the S_0* spectrum in terms of a time-dependent change of the amplitude in the hot band region with the same S_0* decay time constants as mentioned above. Fig. 5 shows a typical S_0* spectrum at 15 ps. In Fig. 8, representative spectra for 13,13′-diphenyl-β-carotene (A) and β-carotene (B) in acetone at 30 ps are displayed which clearly

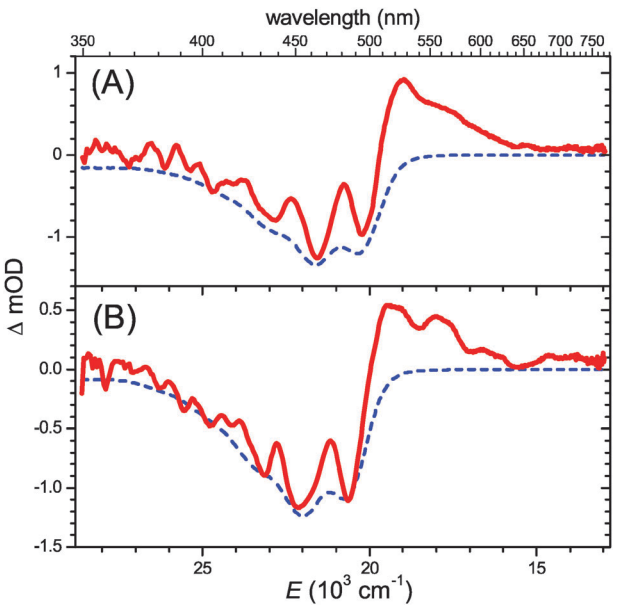

Fig. 7 Transient PSCP absorption spectra in acetone at long times bearing the spectral signature of not yet fully relaxed S_0* molecules (red lines) for (A) 13,13′-diphenyl-β-carotene and (B) β-carotene. Each spectrum was the result of averaging PSCP spectra (Fig. 3 and 4) over the time range 45–60 ps. For comparison, the steady-state absorption spectra (blue dashed lines) were inverted and rescaled.

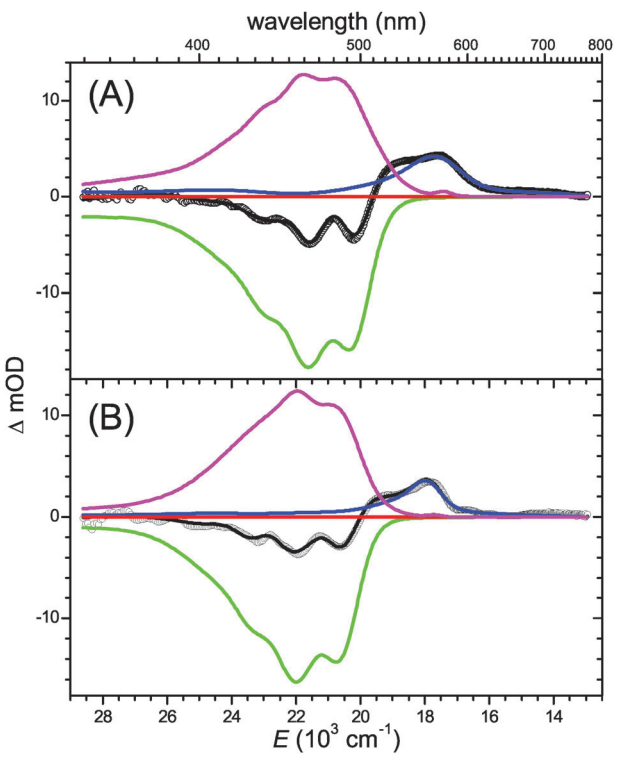

Fig. 8 Result of the global kinetic analysis for the transient PSCP spectrum in acetone (open circles) at 30 ps for (A) 13,13′-diphenyl-β-carotene and (B) β-carotene. Simulation result (black line) with individual contributions from S_1 (blue line), S_0* (magenta line), S_0 (green line), and S_2 (red line).

show how the individual contributions of S_1, S_0* and S_0 add up to the resulting PSCP spectrum, leading to the characteristic strongly modulated bleach structure and the S_0* shoulder to the blue of the S_1 absorption. In the context of these findings we also consider earlier studies of Motzkus and co-workers.[14,15] They suggested that S* in β-carotene homologues is the vibrationally excited S_0 state, which is generated by impulsive stimulated Raman scattering (ISRS) *via* S_2. In our experiments, such an ISRS mechanism would instantaneously generate S_0* carotenes with low vibrational excess energy (*ca.* 1000 cm^{-1}). This excess energy is expected to be quickly dissipated by collisions with the solvent, and certainly much more quickly than for molecules following the $S_2 \rightarrow S_1 \rightarrow S_0^* \rightarrow S_0$ pathway. The latter ones start relaxing in the vibrational S_0 manifold with much higher initial energy. We thus conclude that the contribution of ISRS-prepared molecules to the "hot" spectral features in Fig. 7 will be negligible, see also below. In addition, we could also find no indications in the PSCP spectra for an instantaneous rise of S_0* features at early times.

4.6 Further support for S* being the vibrationally hot ground electronic state S_0*

We believe that we have accumulated comprehensive evidence that S* is indeed the vibrationally excited ground electronic state S_0*. In another key study, we have measured temperature-dependent steady-state absorption spectra $OD(\lambda,T)$ for β-carotene in *n*-hexane solution.[6] From these we could directly extract differential absorption spectra $\Delta OD(\lambda,\langle E\rangle)$ of vibrationally excited β-carotene molecules in S_0 with well-defined average vibrational excess energies $\langle E\rangle$ up to 2144 cm^{-1}. These differential spectra bear all features assigned to the S* state in ultrafast transient absorption experiments, namely an increased absorption on the red edge of the room-temperature $S_0 \rightarrow S_2$ absorption as well as a strongly modulated structure in the bleach region. Both types of features can be easily understood, because additional vibrational excitation leads to a decrease of band peaks, an increase of absorption valleys as well as considerable broadening on the red band edge. As shown above, exactly the same spectral signatures are found in the transient differential spectra of ultrafast PSCP experiments of β-carotene derivatives in solution at long delay times, when IC from S_1 has largely ceased and most of the molecules are in S_0. The same signatures are also present in the transient spectra at earlier times (with larger amplitude),[6] which suggests that they are due to S_0* molecules, originally formed with $\geq$ 14 500 cm^{-1} excess energy[3] upon IC from S_1. Signatures of hot S_0* molecules have been first noticed by Andersson and Gillbro, see *e.g.* their Fig. 5b and 6b in ref. 13. Later on, Motzkus and co-workers, employing much shorter pump pulse durations, demonstrated the presence of S_0* state molecules and proposed the aforementioned ISRS pathway for their formation.[14,15] Very recently, Materny and co-workers have identified S_0* relaxation of β-carotene in benzene by pump-DFWM spectroscopy with a time constant of 12.7 ps, in good agreement with our value of 11.9 ps in *n*-hexane. It is however important to note that very recent studies have argued against the assignment of S* to the vibrationally hot ground electronic state.[11,12,17] It is therefore necessary to discuss these experiments in the following and show that they do *not* contradict our S_0* assignment.

We start with the study of Larsen and co-workers:[12a] They found that narrowband (50 cm^{-1}) and broadband excitation (1000 cm^{-1}) of β-carotene in 3-methylpentane leads to indistinguishable transient spectra. On that basis, Larsen *et al.* ruled out that an ISRS mechanism can be operative. We can easily estimate the expected change in optical density in their experiments based on our previously-recorded temperature-dependent steady-state absorption spectra (magenta and red lines in Fig. 1 of ref. 6): Adding an excess energy of 1000 cm^{-1} (Larsen's broadband case) to the *entire* room-temperature population will result in a change in OD of about 1%. Now an ISRS process can only dump a fraction of the molecules back to the ground electronic state. Estimating an ISRS efficiency of 10% in their experiments, we arrive at a change in OD of 10^{-3} due to the ISRS contribution, so *e.g.* 0.1 mOD for a bleach of 100 mOD in a transient absorption experiment. Such a small change will be undetectable when considering the overlap with other spectral features appearing in this wavelength region such as $S_2 \rightarrow S_0$ stimulated emission, carotenoid and solvent Raman contributions at early times and the quickly-growing strong $S_1 \rightarrow S_n$ absorption at later times. That means that the 1000 cm^{-1} wide pump pulse in Larsen's study is simply spectrally not broad enough to induce any appreciable ISRS contribution.

In the same study, Larsen and co-workers also argued that formation of S_0* by IC from S_1 can be discarded on the basis of previous pump–deplete–probe experiments of the van Grondelle group.[58] We first note that the data presented in Fig. 5 of their paper, which is taken for their main argument of "near-uniform depletion", actually show the opposite: for the given normalization in that paper about 35% depletion in the bleach (450 nm), 10% depletion in the "S* shoulder" (530 nm) and even *no* depletion at the peak of the S_1 absorption (550 nm). Secondly, it is well-known that the SE of C_{40} carotenoids in the region of the dump pulse (550 nm) is overlapped by $S_2 \rightarrow S_n$ absorption,[6,11,22] so the experiment is certainly not a pure pump–deplete–probe but at the same time also a pump–repump–probe experiment. Repumping S_2 population will access higher S_n states which either quickly relax to S_1 or might even partially lead to ionization of the carotenoid,[59,60] both distorting the transient spectra. Also, following up on the argument based on our steady-state absorption spectra in the ISRS case above, an excess energy of 6800 cm^{-1} for their dumped population corresponds to a change of *ca.* 10% in OD if *all* the population would be dumped. Unfortunately, the actual fraction of dumped molecules was not specified by Larsen *et al.* so if we assume again a fraction of 10%, then we end up with a change in OD of 10^{-2} (*e.g.* 1 mOD for an initial bleach of 100 mOD) which will be the gain of S* population by dumping, again too small to be detected in the experiment. Taking all of these arguments together, it is clear that the data of Larsen's group do not contradict the assignment of S* to S_0*.

In another experiment, Christensson *et al.* performed two-dimensional electronic spectroscopy of β-carotene in benzonitrile.[11] Results were interpreted in terms of a model assuming a kinetic scheme, where branching from S_2 populates

the two distinct electronic states S_1 and S*. Both states were assumed to be populated with the *same time constant* of 150 fs. A kinetic model considering S* preparation as a hot ground state by IC from S_1 was not taken into account. Unfortunately, the 2D technique in that specific implementation correlated only a narrow spectral range (508–588 nm), which is roughly one-sixth of the energy range covered in the current and previous PSCP experiments.[6,37] Most importantly, the complete bleach region from 350–500 nm containing the characteristic bleach structure was not covered by the 2D study. However, the spectral features in this region actually provide the key arguments for assigning S* as the hot ground state species S_0* formed by IC from S_1. We also note that the 2D transient spectra were only recorded up to a delay time of 400 fs, so the fairly slow build-up of S_0* *via* IC from S_1 (see our Fig. 6) could not be detected. Our PSCP data suggest that in this early time range the ESA in this spectral region is strongly dominated by S_1. This is actually consistent with the finding of the 2D study that all spectral ESA features in this region increase with the same time constant of roughly 150 fs, which is at the same time in agreement with our 160 fs IC time for $S_2 \rightarrow S_1$. Therefore, we see no contradiction between the 2D data and our assignment of S* to S_0*. It is desirable that future 2D experiments can be extended to a considerably wider wavelength range with an additional analysis of such data in the framework of the S_0*-based model applied in our current study.

Most recently, Holzwarth and co-workers reported transient absorption experiments for β-carotene in several solvents.[17] They assigned S* time constants >10 ps from previous studies to impurities, yet, the sample purity in their study appears to be comparable to *e.g.* that in Frank's and our experiments, when inspecting the very low absorption in the *cis*-peak region in all these experiments.[6,8] Unfortunately, the transient pump–probe spectra in the range 470–700 nm of Holzwarth's study suffer from limited spectral coverage in the GSB region. Therefore, similar to the case of the 2D experiments, an analysis of the important bleach region from 470 nm down to 350 nm is missing in their study. Once again, it must be emphasized that this region provides the key spectral fingerprints for identifying S* as the vibrationally hot ground electronic state S_0* both in steady-state and ultrafast transient absorption experiments. Finally, a simplified sequential relaxation scheme was employed in Holzwarth's study, which *e.g.* does not include IC from vibrationally unrelaxed S_1* states to S_0 (see Section 4.3). Taking all these arguments into account, it is understandable that direct detection of S_0* was not possible in Holzwarth's experiments.

4.7 Impact of phenyl ring substitution at the polyene backbone of β-carotene—Comparison with DFT/TDDFT-TDA calculations

We would finally like to answer the question why 13,13′-diphenyl-β-carotene and β-carotene show similar photophysical properties, specifically a small difference of the $S_0 \rightarrow S_2(0–0)$ transition energy and comparable $S_1 \rightarrow S_0$* IC time constants suggesting similar S_1–S_0 energy gaps. The interpretation is aided by our calculations. We note that TDDFT treatments only consider singly excited configurations, although in polyenes a substantial amount of double excitation character is present, see *e.g.* the discussion in ref. 32. At present, it is hard to judge, how severely this approximation affects the results. The application of more sophisticated methods to the systems of the current work (*e.g.* extended-ADC(2), see ref. 32) is however currently out of reach.

For S_0 we find that both carotenes feature an *s-cis* orientation of the two β-ionone rings with a dihedral angle (5–6–7–8) of 45.9° for 13,13′-diphenyl-β-carotene and 46.6° for β-carotene. The angle of each phenyl plane with respect to the plane of the polyene system at the respective part of the backbone is 111°. The tilt angle of the two phenyl planes with respect to each other is 44.4°. We also calculated energy profiles for phenyl rotation in the ground and excited electronic states. Results for S_0, S_1 and S_2 are included in the ESI‡ (Fig. S3). In all states the potential is rather shallow and increases steeply toward 0 and 180°, reaching barrier heights of *ca.* 40–50 kJ mol^{-1}. There is an additional barrier around 90° which is very small in S_0 (*ca.* 0.8 kJ mol^{-1}) and a bit larger in S_1 (4.3 kJ mol^{-1}) and S_2 (5.3 kJ mol^{-1}). In a 300 K experiment in solution, both phenyl rings will therefore show larger amplitude librations, but they will not be able to surmount the barriers at 0° and 180°. In the S_0 minimum energy structure, the phenyls are slightly tilted toward the plane of the polyene system, suggesting a minor amount of stabilization through conjugation. Consequently, we ascribe the small barrier at 90° in S_0, S_1 and S_2 to a loss of stabilization because the weak extension of the conjugation onto the phenyl rings is broken. Also, a tilt toward 0° and 180° is not favorable due to steric repulsions with the H atoms at the polyene chain. We note that at 90° the difference in barrier height between the S_0 and S_2 states is on the same order as the observed red-shift of the experimental electronic absorption bands of 13,13′-diphenyl-β-carotene relative to β-carotene. It is therefore reasonable to assume that this effect is mostly due to a slightly larger "effective conjugation length" in the excited states of the diphenyl derivative.

The S_0 structure also explains the characteristic experimental ^{1}H-NMR up-field shifts for the protons adjacent to the phenyl rings (see Fig. S1 and Table S1 in the ESI‡). These are caused by the close-to-perpendicular configuration of the phenyl ring planes with respect to the polyene backbone resulting in a ring-current effect.

The predicted difference for the $S_0 \rightarrow S_2$ transition energy of β-carotene and the diphenyl derivative is 147 cm^{-1} (BLYP), 367 cm^{-1} (B3LYP) and 160 cm^{-1} (SVWN), see Table 2 and Tables S3 and S4 in the ESI,‡ compared to the extrapolated experimental gas-phase value of *ca.* 400 cm^{-1}. While the experimental value is underestimated by all three methods, the qualitative trend of observing a weak red-shift (in agreement with experiment) is obviously independent of the functional used, and therefore very robust.

The calculated oscillator strength ratio (13,13′-diphenyl-β-carotene : β-carotene) for this transition varies between 1.05 : 1 (BLYP, SVWN) and 1 : 1 (B3LYP). In the experiment, one finds *ca.* 0.8 : 1, so the trend is different. The reason for this is not entirely clear. Closer inspection of the calculated oscillator strength for the $S_0 \rightarrow S_2$ transition shows that it is reduced by up to 10% when configurations with more strongly

Table 2 Gas-phase transition energies E, transition wavelengths λ and oscillator strengths f from TDDFT-TDA calculations (B3LYP 6-31+G*) for the first five excited singlet states of 13,13′-diphenyl-β-carotene and β-carotene. Note that in the case of the B3LYP functional, the bright $1^1B_u^+$ state ("S_1") is energetically below the dark $2^1A_g^-$ state ("S_2"), compare *e.g.* also ref. 63. BLYP and SVWN provide the correct ordering (see ESI‡)

	13,13′-diphenyl-β-carotene			β-carotene		
State	E/eV	λ/nm	f	E/eV	λ/nm	f
S_1	2.34	530	5.4	2.39	520	5.4
S_2	2.59	479	0.0	2.63	471	0.0
S_3	3.21	386	0.3	3.27	379	0.4
S_4	3.39	365	0.0	3.45	359	0.0
S_5	3.52	352	0.1	3.69	336	0.3

tilted phenyl rings are sampled due to thermal motion. The remaining difference might be a result of the general shortcoming of the TDDFT calculations, which only account for singly excited configurations, whereas these systems are known to possess substantial double excitation character.[32]

Detachment–attachment electron density plots[61] for 13,13′-diphenyl-β-carotene are shown in Fig. 9 for the five lowest excited singlet states (BLYP), for a listing of transition energies and oscillator strengths see Table S3. Results for the B3LYP and SVWN functionals can be found in Table 2 and Table S4 (ESI‡). The plots suggest that for the S_1 and S_2 states electron density is mainly rearranged within the polyene

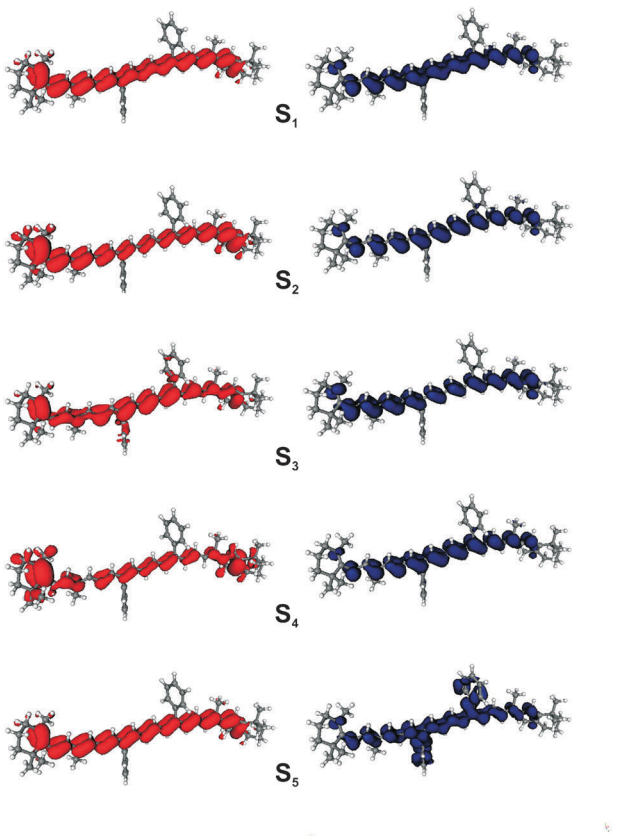

Fig. 9 Detachment (red) and attachment (blue) electron density plots for the lowest five excited singlet states of 13,13′-diphenyl-β-carotene (BLYP functional).

π-system. Using a lower cut-off value for plotting the isosurfaces in Fig. 9 shows that a very small amount of electron density is transferred to the two phenyl rings. A pronounced involvement of the two phenyls is observed only starting from S_5. It is therefore understandable why phenyl substitution at the polyene backbone has a rather small influence on the $S_0 \rightarrow S_2$ steady-state absorption spectrum and the $S_2 \rightarrow S_1$ and $S_1 \rightarrow S_0$* IC dynamics.

We also note that the IC processes from S_2 and S_1 are believed to proceed *via* conical intersections:[62] The "bond-alternation coordinate" (lengthening of C=C bonds and shortening of C–C bonds) of the carotene backbone is likely involved. Such an internal adjustment of the polyene bond lengths neither changes the overall "molecular size" nor does it require large amplitude motions such as torsions. In addition, a second coordinate is needed for the conical intersection, which is likely a local planar distortion, again requiring relatively small geometry alterations.[62] Therefore, large amplitude motions of the phenyl substituents are probably less important.

Finally, it should be mentioned that the transition energies are in reasonable agreement with data for related C_{40} carotenoids, such as zeaxanthin, having the same type of backbone conjugation.[63]

5. Conclusions

We have presented a comprehensive study of a newly-synthesized artificial β-carotene derivative, in which the methyl groups at the 13- and 13′-positions of the polyene chain were replaced by phenyl rings. We note that these type of phenyl substituted carotenes have a particular high thermal stability and can be stored at 0 °C under an inert gas atmosphere for one year without evidence for *trans–cis* isomerization or decomposition. Obviously the additional steric congestion makes isomerization processes more difficult. The impact of this substitution on the photophysical properties is fairly weak: a small (*ca.* 400 cm^{-1}) red-shift of the $S_0 \rightarrow S_2$ steady-state and $S_1 \rightarrow S_n$ transient absorption spectra, basically no change in the $S_2 \rightarrow S_1$ and $S_1 \rightarrow S_0$* internal conversion time constants, much faster IVR time constants for the hot S_1 state and also the presence of the S* "state". The S* difference absorption spectrum shows very sharp bleach and broad absorption features which must be assigned to the absorption of vibrationally hot S_0* molecules on top of a bleach generated by the originally excited S_0 molecules at room temperature. The S_0* cooling time constant of 13,13′-diphenyl-β-carotene is close to that of β-carotene (Table 1) and does not very appreciably in the solvents studied. We have discussed in detail why this interpretation is in agreement with the existing literature on S*.

As highlighted by the DFT/TDDFT-TDA calculations, all the experimental findings can be consistently explained by the close-to-perpendicular orientation of the two phenyl rings with respect to the polyene backbone. As a result, only a small amount of electron density is transferred to the phenyl groups in the energetically lowest electronically excited states S_1 and S_2, leaving them mostly in a spectator role of the photoinduced dynamics in the conjugated polyene backbone. This behavior

might open up interesting applications of these types of molecules as thermally stable building blocks for longer conjugated systems such as conducting molecular wires, where the photophysical properties are approximately retained. Such systems are being currently developed and characterized.[18]

Acknowledgements

We would like to thank N.P. Ernsting and J.L. Pérez Lustres for extensive help during the implementation of the PSCP setup, J. Troe and A.M. Wodtke for on-going generous support, as well as R. Bürsing for excellent technical assistance during the experiments. We are also grateful to A. Düfert and R. Machinek for the characterization of samples by NMR. We thank A. Dreuw for discussions on TDDFT calculations. This work was partly supported by Mid-career Research Program (No. R01-2008-000-20011-0) and by Priority Research Centers Program (No. 2010-0028300) both through the National Research Foundation of Korea funded by the Ministry of Education, Science and Technology. Finally, we also thank the referees for their valuable comments.

Notes and references

1 *The Photochemistry of Carotenoids*, ed. H. A. Frank, A. J. Young, G. Britton and R. J. Cogdell, Kluwer, Dordrecht, 1999, vol. 8, p. 399.
2 H. Ernst, *Pure Appl. Chem.*, 2002, **74**, 2213.
3 T. Polívka and V. Sundström, *Chem. Rev.*, 2004, **104**, 2021.
4 T. Polívka and V. Sundström, *Chem. Phys. Lett.*, 2009, **477**, 1.
5 P. Chabéra, M. Fuciman, P. Hríbek and T. Polívka, *Phys. Chem. Chem. Phys.*, 2009, **11**, 8795.
6 T. Lenzer, F. Ehlers, M. Scholz, R. Oswald and K. Oum, *Phys. Chem. Chem. Phys.*, 2010, **12**, 8832.
7 C. C. Gradinaru, J. T. M. Kennis, E. Papagiannakis, I. H. M. van Stokkum, R. J. Cogdell, G. R. Fleming, R. A. Niederman and R. van Grondelle, *Proc. Natl. Acad. Sci. U. S. A.*, 2001, **98**, 2364.
8 D. M. Niedzwiedzki, J. O. Sullivan, T. Polívka, R. R. Birge and H. A. Frank, *J. Phys. Chem. B*, 2006, **110**, 22872.
9 D. Niedzwiedzki, J. F. Koscielecki, H. Cong, J. O. Sullivan, G. N. Gibson, R. R. Birge and H. A. Frank, *J. Phys. Chem. B*, 2007, **111**, 5984.
10 H. Cong, D. M. Niedzwiedzki, G. N. Gibson and H. A. Frank, *J. Phys. Chem. B*, 2008, **112**, 3558.
11 N. Christensson, F. Milota, A. Nemeth, J. Sperling, H. F. Kauffmann, T. Pullerits and J. Hauer, *J. Phys. Chem. B*, 2009, **113**, 16409.
12 (*a*) A. E. Jailaubekov, S.-H. Song, M. Vengris, R. J. Cogdell and D. S. Larsen, *Chem. Phys. Lett.*, 2010, **487**, 101; (*b*) A. E. Jailaubekov, M. Vengris, S.-H. Song, T. Kusumoto, H. Hashimoto and D. S. Larsen, *J. Phys. Chem. A*, 2011, DOI: 10.1021/jp1082906.
13 P. O. Andersson and T. Gillbro, *J. Chem. Phys.*, 1995, **103**, 2509.
14 W. Wohlleben, T. Buckup, H. Hashimoto, R. J. Cogdell, J. L. Herek and M. Motzkus, *J. Phys. Chem. B*, 2004, **108**, 3320.
15 T. Buckup, J. Savolainen, W. Wohlleben, J. L. Herek, H. Hashimoto, R. R. B. Correia and M. Motzkus, *J. Chem. Phys.*, 2006, **125**, 194505.
16 V. Namboodiri, M. Namboodiri, G. Flachenecker and A. Materny, *J. Chem. Phys.*, 2010, **133**, 054503.
17 E. E. Ostroumov, M. G. Müller, M. Reus and A. R. Holzwarth, *J. Phys. Chem. A*, 2011, DOI: 10.1021/jp105385c.
18 J. Maeng, S. B. Kim, N. J. Lee, E. Choi, S.-Y. Jung, I. Hong, S.-H. Bae, J. T. Oh, B. Lim, J. W. Kim, C. J. Kang and S. Koo, *Chem.–Eur. J.*, 2010, **16**, 7395.
19 S. K. Guha and S. Koo, *J. Org. Chem.*, 2005, **70**, 9662.
20 S. A. Kovalenko, A. L. Dobryakov, J. Ruthmann and N. P. Ernsting, *Phys. Rev. A*, 1999, **59**, 2369.
21 A. L. Dobryakov, S. A. Kovalenko, A. Weigel, J. L. Pérez-Lustres, J. Lange, A. Müller and N. P. Ernsting, *Rev. Sci. Instrum.*, 2010, **81**, 113106.
22 T. Lenzer, S. Schubert, F. Ehlers, P. W. Lohse, M. Scholz and K. Oum, *Arch. Biochem. Biophys.*, 2009, **483**, 213.
23 J. Piel, M. Beutter and E. Riedle, *Opt. Lett.*, 2000, **25**, 180.
24 E. Riedle, M. Beutter, S. Lochbrunner, J. Piel, S. Schenkl, S. Spörlein and W. Zinth, *Appl. Phys. B: Lasers Opt.*, 2000, **71**, 457.
25 K. Oum, P. W. Lohse, F. Ehlers, M. Scholz, M. Kopczynski and T. Lenzer, *Angew. Chem., Int. Ed.*, 2010, **49**, 2230.
26 A. D. Becke, *J. Chem. Phys.*, 1993, **98**, 5648.
27 E. Runge and E. K. U. Gross, *Phys. Rev. Lett.*, 1984, **52**, 997.
28 A. Dreuw and M. Head-Gordon, *Chem. Rev.*, 2005, **105**, 4009.
29 S. Hirata and M. Head-Gordon, *Chem. Phys. Lett.*, 1999, **314**, 291.
30 (*a*) A. D. Becke, *Phys. Rev. A: At., Mol., Opt. Phys.*, 1988, **38**, 3098; (*b*) J. C. Slater, *Quantum Theory of Molecules and Solids*, The Self-Consistent Field for Molecules and Solids, McGraw-Hill, New York, 1st edn, 1974, vol. 4; (*c*) S. H. Vosko, L. Wilk and M. Nusair, *Can. J. Phys.*, 1980, **58**, 1200.
31 Y. Shao, L. Fusti-Molnar, Y. Jung, J. Kussmann, C. Ochsenfeld, S. T. Brown, A. T. B. Gilbert, L. V. Slipchenko, S. V. Levchenko, D. P. O'Neill, R. A. Distasio Jr., R. C. Lochan, T. Wang, G. J. O. Beran, N. A. Besley, J. M. Herbert, C. Y. Lin, T. Van Voorhis, S. H. Chien, A. Sodt, R. P. Steele, V. A. Rassolov, P. E. Maslen, P. P. Korambath, R. D. Adamson, B. Austin, J. Baker, E. F. C. Byrd, H. Dachsel, R. J. Doerksen, A. Dreuw, B. D. Dunietz, A. D. Dutoi, T. R. Furlani, S. R. Gwaltney, A. Heyden, S. Hirata, C.-P. Hsu, G. Kedziora, R. Z. Khalliulin, P. Klunzinger, A. M. Lee, M. S. Lee, W. Liang, I. Lotan, N. Nair, B. Peters, E. I. Proynov, P. A. Pieniazek, Y. M. Rhee, J. Ritchie, E. Rosta, C. D. Sherrill, A. C. Simmonett, J. E. Subotnik, H. L. Woodcock III, W. Zhang, A. T. Bell, A. K. Chakraborty, D. M. Chipman, F. J. Keil, A. Warshel, W. J. Hehre, H. F. Schaefer III, J. Kong, A. I. Krylov, P. M. W. Gill and M. Head-Gordon, *Phys. Chem. Chem. Phys.*, 2006, **8**, 3172.
32 J. H. Starcke, M. Wormit, J. Schirmer and A. Dreuw, *Chem. Phys.*, 2006, **329**, 39.
33 P. O. Andersson, T. Gillbro, L. Ferguson and R. J. Cogdell, *Photochem. Photobiol.*, 1991, **54**, 353.
34 H. Nagae, M. Kuki, R. J. Cogdell and Y. Koyama, *J. Chem. Phys.*, 1994, **101**, 6750.
35 Z. Chen, C. Lee, T. Lenzer and K. Oum, *J. Phys. Chem. A*, 2006, **110**, 11291.
36 R. L. Christensen, M. Goyette, L. Gallagher, J. Duncan, B. DeCoster, J. Lugtenburg, F. J. Jansen and I. van der Hoef, *J. Phys. Chem. A*, 1999, **103**, 2399.
37 J. L. Pérez Lustres, A. L. Dobryakov, A. Holzwarth and M. Veiga, *Angew. Chem., Int. Ed.*, 2007, **46**, 3758.
38 F. L. de Weerd, I. H. M. van Stokkum and R. van Grondelle, *Chem. Phys. Lett.*, 2002, **354**, 38.
39 D. Schwarzer, J. Troe, M. Votsmeier and M. Zerezke, *J. Chem. Phys.*, 1996, **105**, 3121.
40 S. A. Kovalenko, R. Schanz, H. Hennig and N. P. Ernsting, *J. Chem. Phys.*, 2001, **115**, 3256.
41 M. Sajadi, T. Obernhuber, S. A. Kovalenko, M. Mosquera, B. Dick and N. P. Ernsting, *J. Phys. Chem. A*, 2009, **113**, 44.
42 U. Hold, T. Lenzer, K. Luther and A. C. Symonds, *J. Chem. Phys.*, 2003, **119**, 11192.
43 M. L. Horng, J. A. Gardecki, A. Papazyan and M. Maroncelli, *J. Phys. Chem.*, 1995, **99**, 17311.
44 S. Amarie, U. Förster, N. Gildenhoff, A. Dreuw and J. Wachtveitl, *Chem. Phys.*, 2010, **373**, 8.
45 D. Kosumi, M. Komukai, H. Hashimoto and M. Yoshizawa, *Phys. Rev. Lett.*, 2005, **95**, 213601.
46 M. Kopczynski, T. Lenzer, K. Oum, J. Seehusen, M. T. Seidel and V. G. Ushakov, *Phys. Chem. Chem. Phys.*, 2005, **7**, 2793.
47 P. Kukura, D. W. McCamant and R. A. Mathies, *J. Phys. Chem. A*, 2004, **108**, 5921.
48 A. N. Macpherson and T. Gillbro, *J. Phys. Chem. A*, 1998, **102**, 5049.
49 E. Ostroumov, M. G. Müller, C. M. Marian, M. Kleinschmidt and A. R. Holzwarth, *Phys. Rev. Lett.*, 2009, **103**, 108302.
50 D. Polli, M. R. Antognazza, D. Brida, G. Lanzani, G. Cerullo and S. De Silvestri, *Chem. Phys.*, 2008, **350**, 45.
51 H. H. Billsten, J. Pan, S. Sinha, T. Pascher, V. Sundström and T. Polívka, *J. Phys. Chem. A*, 2005, **109**, 6852.

52 H. H. Billsten, D. Zigmantas, V. Sundström and T. Polívka, *Chem. Phys. Lett*., 2002, **355**, 465.
53 D. W. McCamant, J. E. Kim and R. A. Mathies, *J. Phys. Chem. A*, 2002, **106**, 6030.
54 G. Cerullo, G. Lanzani, M. Zavelani-Rossi and S. De Silvestri, *Phys. Rev. B: Condens. Matter Mater. Phys*., 2001, **63**, 241104.
55 D. J. Nesbitt and R. W. Field, *J. Phys. Chem*., 1996, **100**, 12735.
56 R. von Benten, A. Charvat, O. Link, B. Abel and D. Schwarzer, *Chem. Phys. Lett*., 2004, **386**, 325.
57 R. von Benten, O. Link, B. Abel and D. Schwarzer, *J. Phys. Chem. A*, 2004, **108**, 363.
58 D. S. Larsen, E. Papagiannakis, I. H. M. van Stokkum, M. Vengris, J. T. M. Kennis and R. van Grondelle, *Chem. Phys. Lett*., 2003, **381**, 733.
59 S. Amarie, J. Standfuss, T. Barros, W. Kühlbrandt, A. Dreuw and J. Wachtveitl, *J. Phys. Chem. B*, 2007, **111**, 3481.
60 P. W. Lohse, F. Ehlers, K. Oum, M. Scholz and T. Lenzer, *Chem. Phys*., 2010, **373**, 45.
61 M. Head-Gordon, A. M. Grana, D. Maurice and C. A. White, *J. Phys. Chem*., 1995, **99**, 14261.
62 W. Fuß, Y. Haas and S. Zilberg, *Chem. Phys*., 2000, **259**, 273.
63 A. Dreuw, *J. Phys. Chem. A*, 2006, **110**, 4592.